Vol 14 No 4, April 2005
1009-1963/2005/14(04)/0709-05

Chinese Physics

© 2005 Chin. Phys. Soc.
and IOP Publishing Ltd

Theoretical analysis of cavity saturation spectroscopy of weak molecular absorbance*

Ma Wei-Guang(马维光)†, Dong Lei(董 磊),
Yin Wang-Bao(尹王保)‡, and Jia Suo-Tang(贾锁堂)

College of Physics and Electronics Engineering, Shanxi University, State key Laboratory of Quantum Optics and Quantum Optics Devices, Taiyuan 030006, China

(Received 15 March 2004; revised manuscript received 23 November 2004)

A theoretical analysis of sub-Doppler molecular saturation spectroscopy by use of a confocal Fabry–Perot (CFP) cavity is presented. The effects of gas pressure, cavity length and mirror reflectivity on the saturation dip amplitude are analysed. Such a treatment can provide the optimum conditions and a guidance for the experiment of saturating the weak molecular absorption lines.

Keywords: CFP cavity, saturation dip, sub-Doppler spectroscopy
PACC: 0760, 3300

1. Introduction

High-resolution absorption spectroscopy is required in precise atomic and molecular spectroscopy, metrological measurements, optical communications and optical frequency standards.[1−7] For atomic spectroscopy, because of its large transition dipole moment many sophisticated sub-Doppler techniques such as selective reflection,[1] ultra-thin gas cell[2,3] and saturation absorption[4] have been applied to the above fields. However, the application of atomic sub-Doppler spectrum in the field of optical frequency standards cannot meet the requirements for many different frequency standards because of limited transitions. Molecules possess abundant rovibration absorption lines and it is difficult for Doppler broadening absorption lines to obtain high frequency stabilization. Thus the sub-Doppler saturation spectroscopy of molecules has attracted the attention of many researchers. However, the transition dipole moment of molecular absorption lines is small so that a high power density is needed to realize the saturation.

Labachelerie *et al*[5] have realized the saturation spectroscopy of weak acetylene absorption lines by introducing a Fabry–Perot (FP) enhanced cavity. It is possible to increase a power density of $1/(1-R)$ inside the cavity, where R is the input mirror reflectivity. Therefore a high finesse cavity enables one to build up the power high enough to saturate the weak rovibrational transitions. Suzumura and Sasada[6] and Mazzotti *et al*[7] have used this method to saturate the overtone bands of methane and carbon dioxide, respectively.

Gagliardi *et al*[8] have provided an approximate theoretical analysis under the condition of a small absorption coefficient and treated the cavity as a planar FP cavity. However, such an approximation is not suitable under general circumstances and yields a relatively large error in practical application. Also, they only analysed the dependence of the contrast between saturation signal and the transmitted absorption signal on the pressure. In this paper we give the detailed computation without any approximation made and analyse the dependence of the saturation signal on pressure, the cavity length and reflectivity of the cavity mirror by use of the CFP cavity model.

2. Theoretical analysis

The FP cavity is widely used in industry and spectroscopic research. However, for the CFP cavity the transmission is insensitive to laser alignment. Thus

*Project supported by Special Grant for Key Programmes of Basic Research at its Earlier Stage, Ministry of Science and Technology, China (Grant No 2002ccc02500).

†E-mail: mwg@sxu.edu.cn; ‡E-mail: ywb65@sxu.edu.cn

a slight misalignment of the input beam will not produce a strong back-reflection to disturb the diode laser operation. So, many research laboratories have used it as a spectroscopic instrument. The basic structure and the typical ray paths are shown in Fig.1. For the CFP cavity, there exist two types of rays in transmission E_{o1}, E_{o2} and two types of rays in reflection E_{r1}, E_{r2}. Here the two types of transmitted rays are mainly considered.

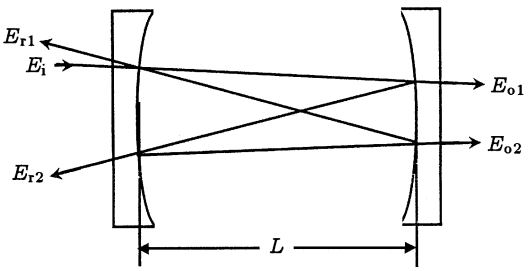


Fig.1. Schematic diagram of a confocal Fabry–Perot cavity and the ray paths.

For a vacuum cavity, the electric field will yield a phase lag of φ_s with respect to that of the initial position when the beam traverses across the cavity length L. Here $\varphi_s = 2\pi nL/\lambda$, n and λ are respectively the refractive index of the cavity medium and optical wavelength. For the successive reflection or the transmission the beam will traverse across the cavity four times. So the phase lag φ is equal to a fourfold φ_s. Using the calculation method which is similar to that for a planar FP cavity and may be found in any optical textbook, the electric field formulae for transmitted rays E_{o1} and E_{o2} are now given by

$$E_{o1} = \frac{(1-R)\exp(-i\varphi_s)}{1-R^2\exp(-i\varphi)}E_i, \tag{1}$$

$$E_{o2} = \frac{R(1-R)\exp(-i3\varphi_s)}{1-R^2\exp(-i\varphi)}E_i. \tag{2}$$

Therefore, the transmitted light intensity I_o can be expressed by

$$\begin{aligned} I_o =& I_{o1} + I_{o2} = E_{o1}E_{o1}^* + E_{o2}E_{o2}^* \\ =& \frac{(1-R)^2 + R^2(1-R)^2}{(1-R^2)^2 + 4R^2\sin^2\varphi/2}I_i. \end{aligned} \tag{3}$$

Under the resonance condition, i.e. $\varphi = 0$, and considering the coupling efficiency between the cavity and laser mode, we can obtain the results as follows:

$$I_o = \eta\frac{(1+R^2)(1-R)^2}{(1-R^2)^2}I_i = \eta\frac{1+R^2}{(1+R)^2}I_i, \tag{4}$$

$$I_c = \frac{I_o}{(1-R)} = \eta\frac{(1+R^2)(1-R)}{(1-R^2)^2}I_i. \tag{5}$$

Here I_i, I_c, I_o are the intensity of incident electric field, electric field inside cavity and electric field output respectively, R is the mirror reflectivity, η is the mode-match parameter.

When there exists an absorption medium in the cavity with an intensity absorption coefficient of $\alpha(\nu)$, the electric field will yield an amplitude attenuation with a coefficient of $\alpha(\nu)/2$ besides the phase lag of φ_s when the beam traverses across the cavity length L. Based on a similar approach to that for the vacuum cavity, the electric field formulae for transmitted rays E'_{o1} and E'_{o2} can be shown to be

$$E'_{o1} = \frac{(1-R)\exp(-i\varphi_s)\exp(-\alpha(\nu)pL/2)}{1-R^2\exp(-i\varphi)\exp(-2\alpha(\nu)pL)}E_i, \tag{6}$$

$$E'_{o2} = \frac{R(1-R)\exp(-i3\varphi_s)\exp(-3\alpha(\nu)pL/2)}{1-R^2\exp(-i\varphi)\exp(-2\alpha(\nu)pL)}E_i. \tag{7}$$

Therefore the transmission intensity with a medium in the cavity can be represented as follows

$$\begin{aligned} I'_o =& I'_{o1} + I'_{o2} = E'_{o1}E'^*_{o1} + E'_{o2}E'^*_{o2} \\ =& \frac{(1+R^2\exp(-2\alpha(\nu)pL))(1-R)^2\exp(-\alpha(\nu)pL)}{(1-R^2\exp(-2\alpha(\nu)pL))^2 + 4R^2\exp(-2\alpha(\nu)pL)\sin^2\varphi/2}I_i. \end{aligned} \tag{8}$$

Also considering the coupling efficiency between the cavity and laser mode and under the resonance condition, the transmitted light intensity can be expressed by

$$I'_o = \eta\frac{(1+R^2\exp(-2\alpha(\nu)pL))(1-R)^2\exp(-\alpha(\nu)pL)}{(1-R^2\exp(-2\alpha(\nu)pL))^2}I_i, \tag{9}$$

where p is the gas pressure of the intra-cavity.

A fraction of change in the transmitted power, caused by the absorbing sample, is deduced from Eqs.(4) and (9) as follows:

$$\Delta I = I_o - I'_o = \eta I_i\left(\frac{1+R^2}{(1+R)^2} - \frac{(1+R^2\exp(-2\alpha(\nu)pL))(1-R)^2\exp(-\alpha(\nu)pL)}{(1-R^2\exp(-2\alpha(\nu)pL))^2}\right). \tag{10}$$

If saturation absorption occurs, a narrow Lamb dip appears at the center of the Doppler broadening profile. The change in the absorption coefficient $\delta\alpha$ due to saturation leads to a variation of the cavity transmission, which is given by

$$\delta I(\delta\alpha) = I'_{\rm o}(\alpha+\delta\alpha) - I'_{\rm o}(\alpha), \tag{11}$$

where δI is just the saturation dip amplitude of absorption line. In the case of small saturation, the value obtained for $\delta\alpha/\alpha$ should be equal to $I_{\rm c}/2I_{\rm s}$.[9] Here $I_{\rm s}$ is the saturation optic intensity and given by[10]

$$I_{\rm s} = \pi\omega_0^2\frac{\varepsilon_0 c\hbar^2}{2\mu^2}10^{12}\left(\frac{C_0}{2}+\frac{C_{\rm p}}{2}p\right)^2. \tag{12}$$

Here ω_0 is the beam waist radius defined by $\sqrt{\frac{L\lambda}{\pi}}$, $\hbar$ is the Planck constant, c is the speed of light, ε_0 is the dielectric constant in vacuum, μ is the dipole moment (C·m), and $C_{\rm p}$ is the pressure broadening coefficient (MHzPa^{-1}). Moreover C_0 is a function of the molecular transit-time through the laser beam and independent of the pressure. It is determined[11] by $\frac{2\pi\sqrt{2k_{\rm B}T}}{8\omega_0\sqrt{M}}$, where $k_{\rm B}$ is the Boltzmann constant, T is the gas temperature (K), M is the mass of single molecule (kg). Using these parameters, Eq.(12) can be simplified to

$$1.098\Omega = C_0 + C_{\rm p}p, \tag{13}$$

where Ω is the Rabi frequency (MHz) and determined by $\frac{1}{2}\mu\times10^{30}\sqrt{\frac{I_s}{\pi\omega_0^2}}$. The terms on the right-hand side of the above equation represent the transit-time broadening linewidth and the pressure broadening linewidth, respectively. Generally, C_0 is so small that it can be ignored. So only when the Rabi frequency is as large as the pressure broadening linewidth, can the saturation phenomenon occur obviously.

Using Eqs.(10) and (11), the contrast G of the sub-Doppler line with respect to the Doppler envelope can be easily calculated as

$$G = \frac{\delta I}{\Delta I}. \tag{14}$$

3. Results and discussion

In order to clearly indicate the results of theoretical analysis, we choose an absorption line of $2\nu_3$ band R (9) manifold (F2-F1 transition) of methane near 6105.6259cm^{-1} as an object. Its basic line parameters[12] are: μ=1.21×10^{-32}C·m, $\alpha(\nu_0)$=3.977×10^{-6}cm^{-1}Pa^{-1}, $C_{\rm p}$=0.02339MHzPa^{-1}, C_0=1.9MHz, $I_{\rm i}$=1.5mW and η= 0.5.

Figure 2 shows the saturation absorption profile which has been simulated by use of Eqs.(10) and (11). The calculation was made on condition that p=50Pa, L=10cm and R=99.2%. Doppler width dominates the absorption line shape at lower pressures. Thus the frequency dependence of $\alpha(\nu)$ can be expressed as $\alpha(\nu_0)\times\exp\left\{-4\ln 2\left(\frac{\nu-\nu_0}{\Delta\nu_D}\right)^2\right\}$ in the calculation. Here ν_0=0 and $\Delta\nu_{\rm D}$ is the Doppler width. The inset in Fig.2 is the magnified section of the part of saturation dip. The contrast G and the linewidth of saturation dip are 30% and 7MHz, respectively. The saturation dip amplitude is about 35μW.

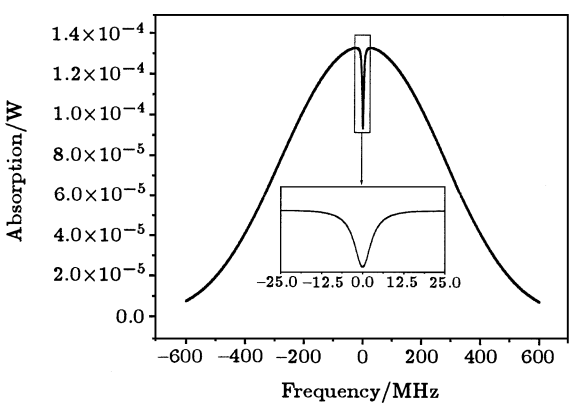


Fig.2. The theoretical saturation absorption spectra on condition that p= 50Pa, L=10cm, R=99.2%. The inset is the magnified section of the middle saturation absorbance. The saturation line width is about 7MHz.

Since the saturation phenomenon is very weak for the weak molecular absorbance, it is necessary to analyse the influence of ambient and instrument conditions on the saturation dip amplitude. Figures 3(a) and (b) represent the saturation dip amplitude and contrast as a function of the pressure on condition that L=10cm and R=99.2%, respectively. Obviously the pressure strongly influences on the saturation dip amplitude and there occurs a maximum at a pressure of 36.24Pa with an amplitude of 42μW. However the contrast decreases continuously with the increasing of pressure. It is interesting to note that the maximum amplitude of saturation dip shifts towards lower pressures with the increasing of L value and simultaneously increases gradually up to a limited value, which is shown in Figs.4(a) and (b), respectively.

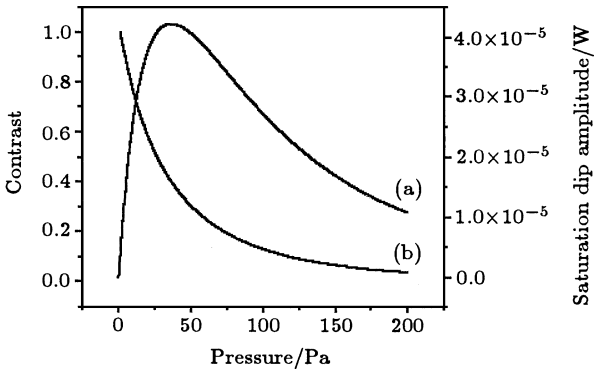


Fig.3. (a) and (b) represent the dependence of the line contrast and the saturation signal on the gas pressure, respectively. The calculation was made on condition that L=10cm, R=99.2%.

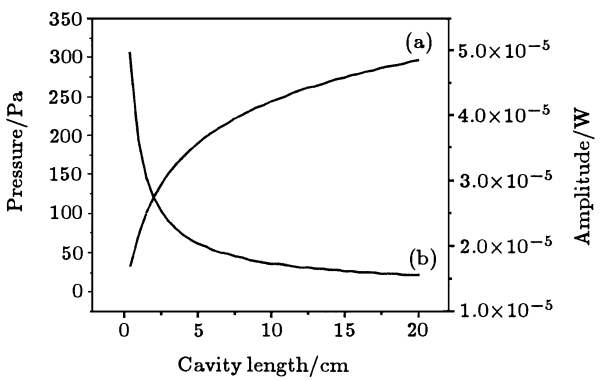


Fig.4. The pressure and the amplitude corresponding to the maximum in Fig.3(a) as a function of cavity length. The calculation was made under the condition of R=99.2%.

Finally, we turn our attention to the features of the optical cavity: the cavity length L and the mirror reflectivity R. The selection of these two parameters is restricted by the alignment of CFP cavity and the machining technology of high reflectivity mirror in the practical application. Figure 5 represents the contour of the dip amplitude with the variations of L and R. Here an arbitrary pressure of 10Pa is adopted. From the figure, we see that the signal amplitude reaches a maximum of 224μW at a length of 0.5 cm and reflectivity of 99.98%. The optimum amplitude shifts towards short cavity length for high mirror reflectivities. However, for long cavity length the optimum amplitude shifts towards the low reflectivity. For each amplitude there exists a series of groups of L and R. While preparing for the experiment, we can adopt a group of parameters of an easy-adjustable cavity to obtain a higher saturation dip amplitude via such a contour. The same holds true for other pressures.

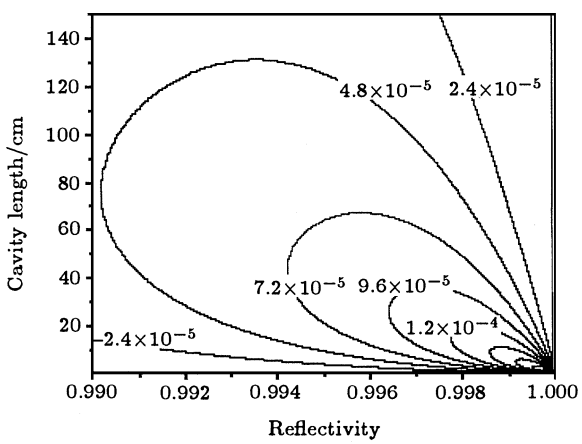


Fig.5. The contour of the saturation dip amplitude as a function of L and R. The amplitude is in units of W.

4. Conclusions

A novel sub-Doppler cavity saturation spectroscopy of molecular weak absorbance is derived by analysing the characteristics of confocal FP cavity and the saturation of weak absorbance. As the pressure increases, the contrast decreases rapidly and there occurs a maximum for the saturation dip amplitude. This maximum shifts towards lower pressure as the cavity length increases. We also present a contour of the dip amplitude as a function of L and R. Such a method can be attractive in high-resolution spectroscopy fields and this analysis can provide the theoretical guidance for the experiment.

References

[1] Chevrollier M, Oria M, Souza J, Bloch D, Fichet M and Ducloy M 2001 *Phys. Rev.* E **63** 046610-1

[2] Briaudeau Stephan, Bloch Daniel and Ducloy Martial 1999 *Phys. Rev.* A **59** 3723

[3] Zhao Y T, Zhao J M, Xiao L T and Jia S T 2003 *Chin. Phys.* **12** 390

[4] Letokhov V and Chebotayev V 1977 *Nonlinear Laser Spectroscopy, Spring Series in Optival Science* (Berlin: Springer) p4

[5] Labachelerie M, Nakagawa K and Ohtsu M 1994 *Opt. Lett.* **19** 840

[6] Suzumura K and Sasada H 1995 *Jpn. J. Appl. Phys.* **34** L1620

[7] Mazzotti D, Natale P, Giusfredi G, Fort C, Mitchell J and Hollberg L 2000 *Opt. Lett.* **25** 350
[8] Gagliardi G, Rusciano F and Gianfrani L 2000 *Appl. Phys.* B **70** 883
[9] Letokhov V 1976 *High-Resolution Laser Spectroscopy, Springer Series in Appl. Phys.* (Berlin: Springer) pp95-199
[10] Shimoda K 1976 *High-Resolution Laser Spectroscopy, Springer Series in Appl. Phys.* (Berlin: Springer) pp1-49
[11] Gianfrani Livio, Fox Richard and Hollberg Leo 1999 *J. Opt. Soc. Am.* B **16** 2247
[12] Rothman L, Barbe A, Benner D, Brown L, Camy-Peyret C, Carleer M, Chance K, Clerbaux C, Dana V, Devi V, Fayt A, Flaud J, Gamache R, Goldman A, Jacquemart D, Jucks K, Lafferty W, Mandin J, Massie S, Nemtchinov V, Newnham D, Perrin A, Rinsland C, Schroeder J, Smith K, Smith M, Tang K, Toth R, Auwera J, Varanasi P and Yoshino K 2003 *J. Quant. Spectrosc. Radiat. Transfer.* **82** 5